http://dx.doi.org/10.21577/0103-5053.20200045

J. Braz. Chem. Soc., Vol. 31, No. 8, 1597-1604, 2020
Printed in Brazil - ©2020 Sociedade Brasileira de Química

Article

Catalytic Dehydration of Glycerol to Acrolein over Aluminum Phosphate Catalysts

Tianlin Ma, [*,#,a] *Jianfei Ding,*[#,b] *Xueli Liu,*[a] *Jiandong Zheng*[a] *and Zhi Yun*[c]

[a]*School of Materials and Chemical Engineering, Chuzhou University, 239000 Chuzhou, P. R. China*

[b]*School of Chemistry and Chemical Engineering, Yancheng Institute of Technology, 224051 Yancheng, P. R. China*

[c]*College of Chemical Engineering, Nanjing Tech University, 210009 Nanjing, P. R. China*

Gas phase conversion of glycerol to acrolein over a variety of aluminum phosphate (AlP) catalysts synthesized by a simple replacement reaction method with a variation in calcination temperature (300-700 °C, AlP-300, AlP-400, AlP-500, AlP-600, and AlP-700, respectively) has been investigated. The textural properties, acidities and coke contents of the samples were also determined. The catalysts were presented in an amorphous state when the AlP sample was calcined below 500 °C. Further increasing the calcination temperature promoted the formation of orthorhombic α-$AlPO_4$ crystal. The weak acid sites increased when the calcination temperature was raised from 300 to 500 °C. However, the weak acid sites decreased when the AlP was calcined above 500 °C. The acidity of the catalyst played a crucial role in the glycerol dehydration reaction. The maximum acrolein selectivity of 66% at 98% glycerol conversion was obtained over AlP-500 catalyst, due to the largest number of acid sites and appropriate textural properties. AlP-700 exhibited the lowest glycerol conversion, owing to the formation of orthorhombic α-$AlPO_4$ crystalline phase and the lowest amount of acid sites under high calcination temperature. The significant reduction in the acidity of the used sample led to a decrease of glycerol conversion.

Keywords: glycerol, acrolein, dehydration, aluminum phosphate

Introduction

Nowadays, biodiesel as an important renewable resource has obtained increasing concern.[1] Glycerol is the major by-product of biodiesel production, which is about 10 wt.% of the total products.[2] The applications of glycerol to valuable products have been a research hotspot so far.[3] Consequently, many researchers[1,4-8] have focused on designing effective catalysts for conversion of glycerol to acrolein, which is applied widely in the production of textiles, polymers, acrylic acid esters and methionine.

Gas-phase conversion of glycerol is generally considered as an environmentally friendly and economical approach. Various solid acid catalysts have been studied in this important reaction, including phosphates,[9] metal oxides,[4,10] zeolites,[7,11] and heteropolyacids.[5,6,12,13] Among these acid catalysts, phosphate catalysts have been widely studied in the glycerol dehydration reaction due to its superior catalytic performance. Suprun *et al.*[14] reported the catalytic activity of H_3PO_4 modified Al_2O_3 and TiO_2 catalysts. The glycerol conversion on Al_2O_3-PO_4 and TiO_2-PO_4 was 100 and 98%, respectively. The acrolein selectivity on Al_2O_3-PO_4 and TiO_2-PO_4 was 42 and 37%, respectively, and the catalysts deactivated slowly. Deleplanque *et al.*[15] obtained 100% glycerol conversion and 92% acrolein selectivity using $FePO_4$ as catalyst. Estevez *et al.*[16] prepared the mesoporous $AlPO_4$ by a simple ammonia sol-gel method. The $AlPO_4$-650 showed the maximum acrolein yield (23%) at 270 °C and 1 bar pressure. Estevez and co-workers[17] also studied the influence of a transition metal (Cu, Co, Cr, Fe) in the dispersion phase of $AlPO_4$, obtaining the maximum acrolein yield (54%) on AlCoPO650. Many studies demonstrated that the catalytic performance was associated with the calcination temperature of the phosphate catalysts. However, the aforementioned papers did not investigate the influence of calcination temperatures on catalyst structure and performance in detail, which could not reveal the property-activity relationship.

In the present paper, aluminum phosphate catalysts were synthesized using a simple replacement reaction method with a variation of calcination temperature (300-700 °C).

*e-mail: matianlin951@sina.com
#These authors contributed equally to this work.

The purpose of this work is to investigate changes in the structure, acidity amount, acidity strength and acid type of the catalysts as a function of calcination temperature and to find the correlation between the surface properties of catalysts and catalytic activities during the glycerol dehydration reaction.

Experimental

Catalyst preparation

All necessary chemicals were purchased from Aladdin Chemistry Co., Ltd. (Shanghai, China), and used without further purification. Aluminum phosphate (AlP) was prepared by a simple replacement reaction method from $Al(NO_3)_3 \cdot 9H_2O$ and $Na_3PO_4 \cdot 12H_2O$. Firstly, 61 g of $Al(NO_3)_3 \cdot 9H_2O$ and 61.8 g of $Na_3PO_4 \cdot 12H_2O$ were added to 350 mL of deionized water in a 500 mL of round-bottom flask under stirring. The solution was stirred at 100 °C for 5 h until no more precipitate formed. After the solution was cooled to room temperature, the solution was filtrated and washed with deionized water twenty times. The solid obtained was dried at 120 °C for 12 h and calcined at different temperatures (300, 400, 500, 600, and 700 °C) for 4 h in a muffle furnace at a heating rate of 5 °C min^{-1} prior to reaction. The resulting material was denoted as AlP-T, where T represented the calcination temperature. For comparison, the AlP sample without calcination was also prepared.

Catalyst characterization

X-ray diffraction (XRD) data was obtained using a Shimadzu XRD-6000 instrument with Cu Kα radiation operated at 40 kV and 40 mA. The specific surface area, pore volume and pore size of catalysts were determined by a Micromeritics ASAP 2020 instrument. Temperature programmed desorption of ammonia (NH_3-TPD) analysis was carried out on a Builder PCA-1200 instrument, and the amount of acid sites was calculated by quantifying the desorbed NH_3 from NH_3-TPD. Fourier transformed infrared spectroscopy (FTIR) of pyridine adsorption experiments were analyzed by a Shimadzu FTIR-8700 spectrometer. The coke content of the used catalysts was obtained for elemental characterization on a CHNS analyzer (Vario EL III).

Catalytic reaction

The catalytic performance of samples was conducted for the dehydration of glycerol using a vertical fixed-bed reactor at atmospheric pressure. The reactor length was 50 cm and its inner diameter was 8 mm. 1 g of catalyst was placed in the middle part of the reactor and quartz wool was put at both ends. Prior to the reaction, the catalyst was pretreated at 280 °C under nitrogen flow (40 mL min^{-1}) for about 1 h. Liquid aqueous glycerol (10 wt.%) was injected by a syringe pump with 0.08 mL min^{-1} flow-rate in a N_2 flow (10 mL min^{-1}). The reaction temperature was fixed at 280 °C for all reactions. After 1 h, the products and unconverted glycerol were condensed in a water-ice mixture and taken hourly for analysis.

The analysis was performed using a gas chromatograph (GC) equipped with a capillary column (HP-INNOWAX; 60 m × 0.32 mm × 0.25 μm) and flame ionization detector (FID) using methanol as an internal standard. Glycerol conversion and product selectivities were defined as follows:

$$\text{Glycerol conversion}(\%) = \frac{\text{Moles of glycerol reacted}}{\text{Moles of glycerol in the feed}} \times 100 \quad (1)$$

$$\text{Product selectivity}(\%) = \frac{\text{Moles of carbon in a product formed}}{\text{Moles of carbon in glycerol consumed}} \times 100 \quad (2)$$

$$\text{Acrolein yield}(\%) = \frac{\text{Glycerol conversion} \times \text{acrolein selectivity}}{100} \quad (3)$$

Results and Discussion

Catalyst characterization

The XRD patterns of AlP and AlP-T catalysts are illustrated in Figure 1. When the AlP catalyst is calcined below 500 °C, there is only a very broad peak between 15-40°, indicating that the catalysts are presented in an amorphous state. On calcination at 600 °C, the characteristic diffraction peaks of the orthorhombic α-$AlPO_4$ crystalline phase at 2θ angles of 20.3, 21.5, 23.0, and 35.6° are appeared.[18] With further raising calcination temperature to 700 °C, the intensities of the XRD diffraction peaks of the orthorhombic α-$AlPO_4$ crystalline phase increase. From the above results, it can be concluded that the $AlPO_4$ remains in an amorphous state when the calcination temperature is lower than 600 °C. Further increasing the calcination temperature facilitates the formation of orthorhombic α-$AlPO_4$ crystalline phase. Similar XRD results on $AlPO_4$ were observed by Liu *et al.*[18] and Mohamed *et al.*[19] Moreover, Lopez-Pedrajas *et al.*[20] found that the amorphous $AlPO_4$ showed higher performance in the glycerol dehydration reaction than the other highly crystalline metal phosphates.

Figure 2 illustrates the N_2 adsorption-desorption isotherms of AlP and AlP-T samples. Figure 3 shows the

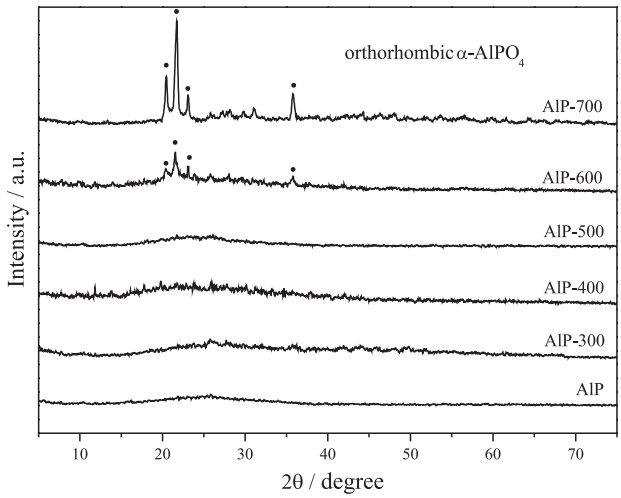

Figure 1. XRD patterns of the AlP and AlP-T samples.

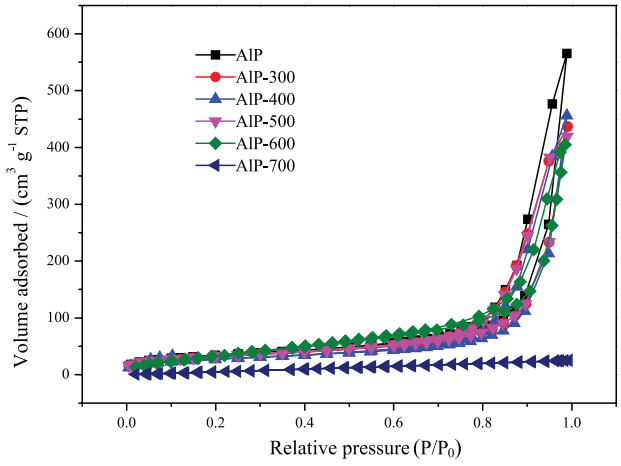

Figure 2. Nitrogen adsorption-desorption isotherms of the AlP and AlP-T samples.

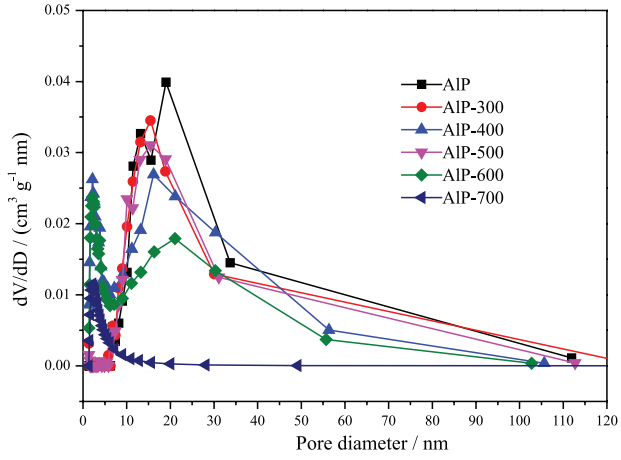

Figure 3. Pore diameter distributions of the AlP and AlP-T samples.

pore diameter distributions of AlP and AlP-T samples. Compared with the AlP, the shape of the isotherm after calcination at 300, 400, 500 and 600 °C does not show obvious change. However, the uptake of the isotherm at a relative pressure higher than 0.8 disappears at 700 °C, indicating the elimination of mesopores, which is due to the formation of orthorhombic α-$AlPO_4$ crystalline phase under high calcination temperature.[18,19] The textural properties of the samples were calculated from N_2 physical adsorption-desorption measurements and the results are listed in Table 1. The surface area decreases when the AlP is calcined from 300 to 500 °C, which is due to large shrinkage.[21] When the AlP is calcined at 600 °C, the surface area immediately increases to 202 $m^2\ g^{-1}$, and then decreases to 52 $m^2\ g^{-1}$ with further raising the calcination temperature. The increase of surface area at 600 °C is attributed to the formation of orthorhombic α-$AlPO_4$ crystal and the decrease of surface area at 700 °C is owing to the growth of nanocrystals and sintering of skeletons. Meanwhile, the pore volume and pore size decrease with increase of calcination temperature, which are similar to the results reported by Mohamed *et al.*[19] and Li *et al.*[21] Moreover, Estevez *et al.*[16] reported that appropriate textural properties could increase the catalytic performance in the dehydration of glycerol to acrolein.

Table 1. Textural properties of the AlP and AlP-T catalysts

Catalyst	Surface area / ($m^2\ g^{-1}$)	Pore volume / ($cm^3\ g^{-1}$)	Pore size / nm
AlP[a]	153	0.89	18.992
AlP-300[a]	141	0.69	15.651
AlP-400[a]	138	0.68	16.122
AlP-500[a]	135	0.66	15.462
AlP-600[a]	202	0.65	2.167
AlP-700[a]	52	0.05	2.164

[a]$AlPO_4$ and $AlPO_4$ calcined at 300, 400, 500, 600, and 700 °C.

The acidity of catalyst measured by NH_3-TPD is an important parameter in glycerol dehydration reaction. The NH_3-TPD profiles of AlP and AlP-T samples are revealed in Figure 4. The strength of acid sites on the sample is proportional to the desorption temperature. The desorption profiles of the catalysts show a broad peak at about 204 °C in the range of 150-350 °C except for the AlP-700 sample, which is due to weak acid sites. Compared to the AlP, AlP-300 catalyst shows more weak acid sites, suggesting that appropriate calcination temperature can increase the acid sites of AlP. The weak acid sites increase when the calcination temperature is increased from 300 to 500 °C, which is due to the occurrence of dehydroxylation including the removal of –OH groups.[21] However, the weak acid sites decrease when the AlP is calcined above 500 °C, probably owing to partial decomposition of weak acid sites and sintering of the AlP. These results

are similar to the findings of Mohamed *et al.*,[19] who reported that the acid value increased with increasing the calcination temperature from 350 to 450 °C. A further increase in the calcination temperature led to a decrease in these acid values. The acidity of the catalysts are in an order of AlP-500 > AlP-400 > AlP-300 > AlP > AlP-600 > AlP-700. It is worth noting that many researchers[6,14,22] reported that the glycerol conversion depended on the acidity of the catalyst.

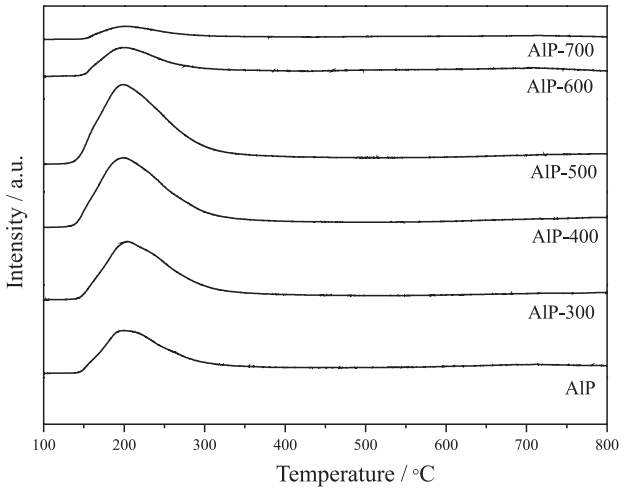

Figure 4. NH_3-TPD profiles of the AlP and AlP-T samples.

Many researchers[6,13,14] reported that Brønsted and Lewis acid sites influenced the product distribution in the glycerol dehydration reaction. Therefore, pyridine-FTIR experiments were conducted to determine the Brønsted and Lewis acid sites. The pyridine-FTIR spectra of AlP and AlP-T samples are shown in Figure 5. The peak at approximately 1448 and 1540 cm^{-1} is due to Lewis and Brønsted acid sites, respectively. The Brønsted and Lewis acid sites are present on AlP, AlP-300, AlP-400 and AlP-500, while AlP-600 and AlP-700 only show Lewis acid sites. The Lewis acid sites increase and the Brønsted acid sites show no obvious change when the calcination temperature is increased to 500 °C. The Lewis acid sites decrease when the AlP is calcined above 500 °C.

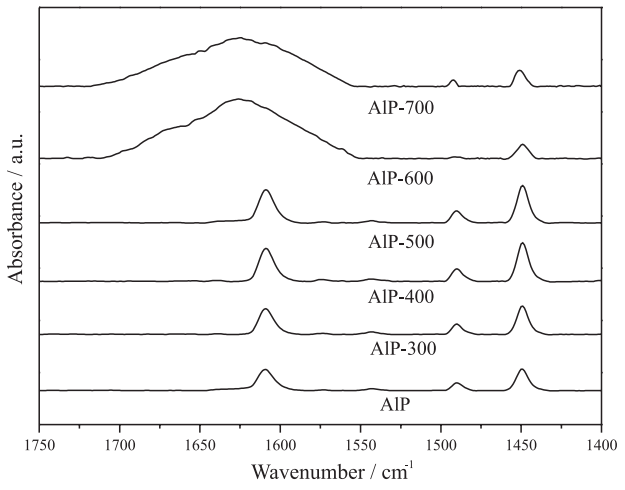

Figure 5. Pyridine-FTIR spectra of the AlP and AlP-T samples.

Catalytic activity

The catalytic results of AlP and AlP-T samples at 280 °C and 2 h reaction time are listed in Table 2. Acrolein is the main product in the dehydration of glycerol over all the catalysts. Moreover, some byproducts including hydroxyacetone, formaldehyde, acetaldehyde and acetic acid are detected. The glycerol conversion (45%) and acrolein selectivity (25%) are very low under blank reaction conditions. The AlP and AlP-T samples show higher glycerol conversion and acrolein selectivity than the blank reaction. When the calcination temperature is raised to 500 °C, the glycerol conversion is enhanced from 87 to 98%, which is proportional to the acidity of samples according to the NH_3-TPD results. The AlP-500 sample gives the highest glycerol conversion of 98%, acrolein selectivity of 66%, and acrolein yield of 65%. This is because AlP-500 has the largest number of acid sites and appropriate textural properties. These results indicate that the catalyst acidity and appropriate textural properties are crucial parameters for obtaining superior results in this reaction, consistent with the previous reports.[16,23] With further raising calcination temperature to 700 °C, the glycerol conversion, acrolein selectivity and acrolein yield decrease. This can be owing to the following reasons: (*i*) the formation of orthorhombic α-$AlPO_4$ crystalline phase under high calcination temperature; (*ii*) changes in the textural properties including decreased surface areas, pore volumes and pore sizes under high calcination temperature; and (*iii*) the decrease of acid sites under high calcination temperature. Moreover, many researchers[6,13,14] found that the Brønsted acid sites were beneficial to produce acrolein. However, the correlation of Brønsted acid sites and acrolein selectivity is not found in this study. In the dehydration of glycerol to acrolein, water is present at a relatively high temperature, some Lewis acidic sites interacting with steam present in the system are converted to Brønsted ones to yield more acrolein.[24]

A comparison of the catalytic performance of different metal phosphate catalysts in the gas phase dehydration of glycerol to acrolein is shown in Table 3. The iron phosphate prepared by hydrothermal method ($FePO_4$-H) showed the best catalytic performance, with 100% glycerol conversion and 92% acrolein yield after 5 h of reaction.[15] The ZrP-400 exhibited lower acrolein yield (81.5%) than $FePO_4$-H.

Table 2. Catalytic performances of the AlP and AlP-T samples at 280 °C and 2 h reaction time

Catalyst	X[a] / %	Y[b] / %	Selectivity / %					
			Acrolein	Hydroxyacetone	Acetaldehyde	Formaldehyde	Acetic acid	Others
Blank	45	11	25	8	6	5	8	48
AlP[c]	87	52	60	14	13	5	2	6
AlP-300[c]	91	53	58	16	14	3	2	7
AlP-400[c]	94	54	57	18	14	3	1	7
AlP-500[c]	98	65	66	11	15	2	2	4
AlP-600[c]	72	45	62	5	20	5	3	5
AlP-700[c]	41	20	49	7	24	4	4	12

[a]Glycerol conversion; [b]acrolein yield; [c]$AlPO_4$ and $AlPO_4$ calcined at 300, 400, 500, 600, and 700 °C.

Meanwhile, it can be seen that AlP-500 prepared by a simple replacement reaction method in this work shows higher catalytic performance than other metal phosphate catalysts except for $FePO_4$-H and ZrP-400.

Figure 6 shows the catalytic performance of AlP and AlP-T samples calcined at different temperatures with time on stream (TOS) at 280 °C. The results show that AlP-500 sample gives the highest glycerol conversion during 6 h of reaction, which can be attributed to that AlP-500 has the largest number of acid sites and appropriate textural properties. AlP-400 shows lower glycerol conversion than AlP-500 during 6 h of reaction. In addition, AlP-700 exhibits the lowest glycerol conversion during 6 h of reaction, attributed to the formation of orthorhombic α-$AlPO_4$ crystalline phase and the decrease of acid sites under high calcination temperature. It is worth noting that glycerol conversion reduces with time on stream, due to the catalyst deactivation by carbon deposition, which is the major cause of deactivation over solid acids catalysts during glycerol dehydration reaction.[1,6] Among the catalysts, AlP-500 shows the highest acrolein selectivity and yield and AlP-700 exhibits the lowest acrolein selectivity and yield during 6 h of reaction. The catalytic results show that there is not significant difference among obtained acrolein selectivities over AlP, AlP-300, AlP-400, and AlP-600, maybe due to their similar textural properties. It is also noticed that acrolein selectivity and yield of the catalysts show no obvious decrease with time on stream. Similar results were reported by dos Santos *et al*.[26] Moreover, the trends of acrolein selectivity and yield of AlP and AlP-T samples calcined at different temperatures are not directly correlated with the trend of total acidities and Brønsted acid sites of the samples.

Time-on-stream studies of the AlP-500

The glycerol conversion and acrolein selectivity change with TOS was investigated over the AlP-500 catalyst at 280 °C (Figure 7). The glycerol conversion reduces from 98 to 80% and the acrolein selectivity keeps relative stable

Table 3. Comparison of catalytic performance of different metal phosphates catalysts in the gas phase dehydration of glycerol to acrolein

Catalyst	Reaction temperature / °C	Reaction time / h	$X_{glycerol}$[a] / %	$S_{acrolein}$[b] / %	$Y_{acrolein}$[c] / %	Reference
Al_2O_3-PO_4	280	1	100	42	42	14
TiO_2-PO_4	280	1	98	37	36	14
$FePO_4$-H	280	5	100	92.1	92.1	15
Ca/HAP	350	2	85	9	7	9
ZrP-400	315	10	100	81.5	81.5	25
$AlPO_4$450	280	3	41	49	20	17
AlCoPO450	280	3	86	51	44	17
AlCuPO450	280	3	77	60	46	17
AlP-500[d]	280	2	98	66	65	this work

[a]Glycerol conversion; [b]acrolein selectivity; [c]acrolein yield; [d]$AlPO_4$ calcined at 500 °C. $FePO_4$-H: iron phosphate prepared by hydrothermal method; HAP: hydroxyapatite; ZrP-400: zirconium phosphate calcined at 400 °C; AlPO4450: aluminum phosphate prepared by sol-gel method calcined at 450 °C; AlCoPO450: adding Co in the dispersion phase of $AlPO_4$ calcined at 450 °C; AlCuPO450: adding Cu in the dispersion phase of AlPO4 calcined at 450 °C.

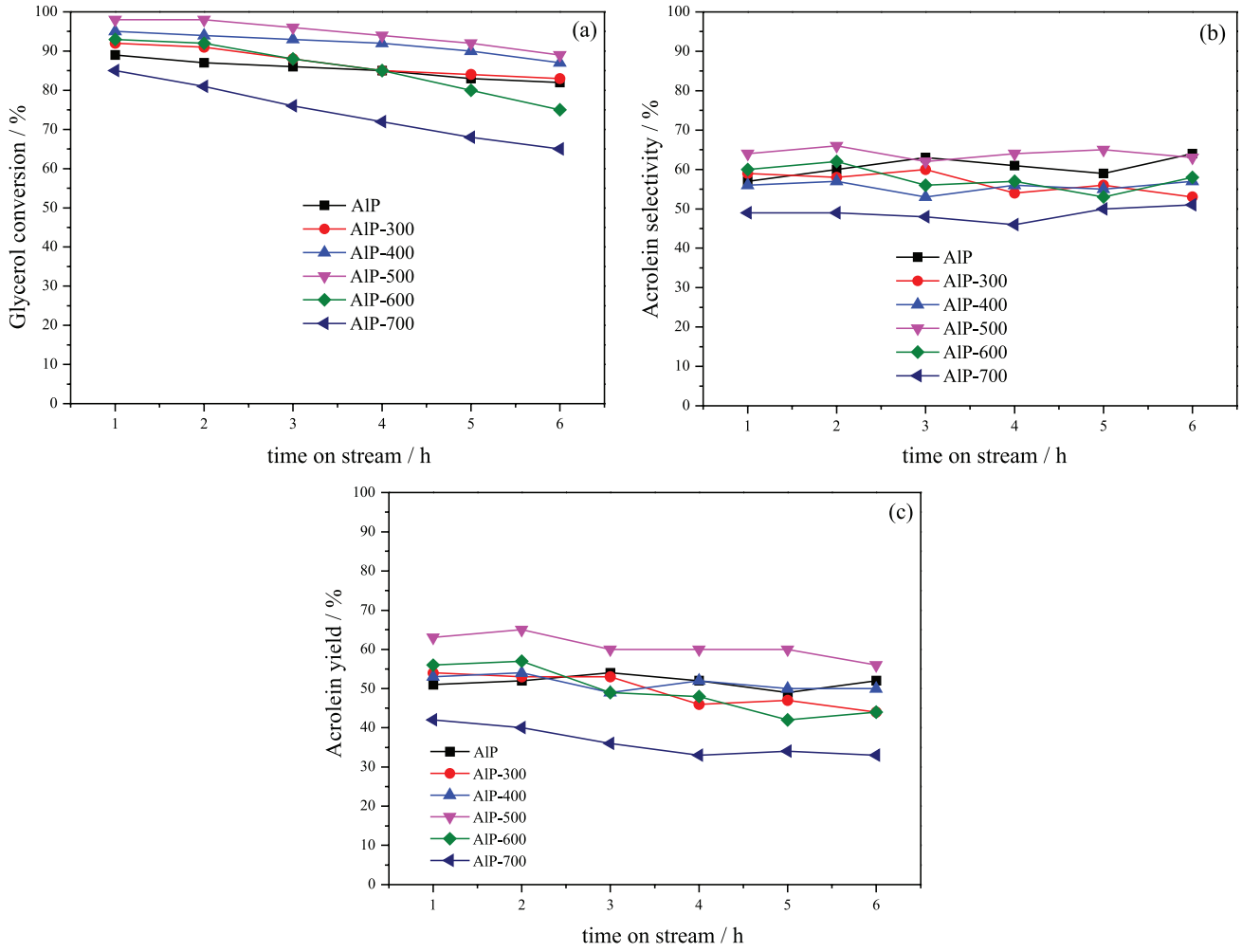

Figure 6. (a) Glycerol conversion; (b) acrolein selectivity; (c) acrolein yield over the AlP and AlP-T samples.

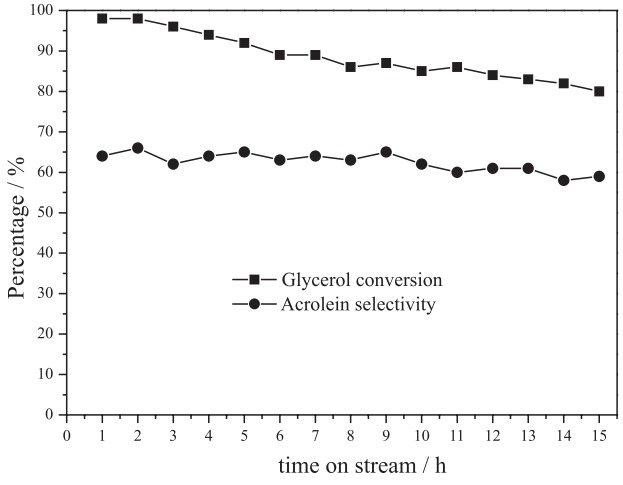

Figure 7. Time-on-stream studies over the AlP-500 catalyst.

after reaction for 15 h. The decrease in glycerol conversion is due to the catalyst deactivation by carbon deposition.[1,6] The coke content of used AlP-500 catalyst was measured by a CHNS analyzer, and about 1.4 wt.% carbon was deposited after 15 h of reaction. The spent AlP-500 after 15 h of reaction was characterized by XRD and NH_3-TPD to study the information about the changes of the structure and acid sites of the catalyst during the reaction. The XRD patterns of the fresh and spent AlP-500 catalysts are shown in Figure 8. The result clearly indicates that the structure of AlP-500 catalyst is maintained after the glycerol dehydration reaction. The NH_3-TPD profiles of the fresh and used AlP-500 catalysts are shown in Figure 9. The used AlP-500 shows fewer acid sites than fresh AlP-500. This result suggests that the decrease of the acidity of AlP-500 caused by carbon deposition reduces the glycerol conversion considerably.

Conclusions

In this work, a series of aluminum phosphates samples were synthesized by a simple replacement reaction method with a variation of calcination temperature for acid catalyzed glycerol dehydration reaction. When the

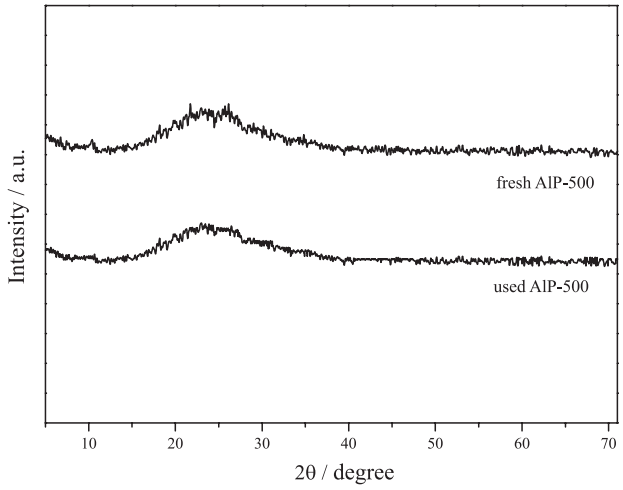

Figure 8. XRD patterns of the fresh and used AlP-500 catalysts.

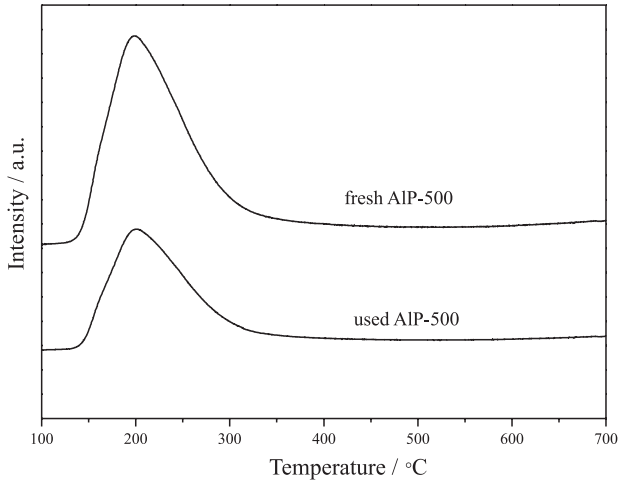

Figure 9. NH_3-TPD profiles of the fresh and used AlP-500 catalysts.

AlP sample was calcined below 500 °C, the catalysts were presented in an amorphous state. Further raising the calcination temperature promoted the formation of orthorhombic α-$AlPO_4$ crystal. The weak acid sites increased when the calcination temperature was raised from 300 to 500 °C, which was ascribed to the occurrence of dehydroxylation including the removal of –OH groups. However, the weak acid sites decreased when the AlP was calcined above 500 °C, probably owing to partial decomposition of weak acid sites and sintering of the AlP. The acidity of the catalyst played a crucial role in the glycerol dehydration reaction. AlP-500 catalyst showed the highest glycerol conversion of 98%, acrolein selectivity of 66%, and acrolein yield of 65%. This was because AlP-500 had the largest number of acid sites and appropriate textural properties. AlP-700 exhibited the lowest glycerol conversion, owing to the formation of orthorhombic α-$AlPO_4$ crystalline phase and the lowest amount of acid sites under high calcination temperature. The significant decrease in the acidity of the spent sample led to a decrease in the glycerol conversion.

Acknowledgments

This work was supported by the University Natural Science Research Key Project of Anhui Province (KJ2018A0435, KJ2017A412), the University Natural Science Research General Project of Anhui Province (KJ2018B15), Scientific Research Start Foundation Project of Chuzhou University (2017qd12 and 2017qd15), and Anhui Provincial Natural Science Foundation (1808085MB50).

References

1. Talebian-Kiakalaieh, A.; Amin, N. A. S.; *Renewable Energy* **2017**, *114*, 794.
2. Anitha, M.; Kamarudin, S. K.; Kofli, N. T.; *Chem. Eng. J.* **2016**, *295*, 119.
3. Chagas, P.; Thibau, M. A.; Breder, S.; Souza, P. P.; Caldeira, G. S.; Portilho, M. F.; Castro, C. S.; Oliveira, L. C. A.; *Chem. Eng. J.* **2019**, *369*, 1102.
4. Chai, S.; Wang, H.; Liang, Y.; Xu, B.; *Green Chem.* **2017**, *9*, 1130.
5. Shen, L.; Yin, H.; Wang, A.; Feng, Y.; Shen, Y.; Wu, Z.; Jiang, T.; *Chem. Eng. J.* **2012**, *180*, 277.
6. Ma, T.; Yun, Z.; Xu, W.; Chen, L.; Li, L.; Ding, J.; Shao, R.; *Chem. Eng. J.* **2016**, *294*, 343.
7. Ren, X.; Zhang, F.; Sudhakar, M.; Wang, N.; Dai, J.; Liu, L.; *Catal. Today* **2019**, *332*, 20.
8. Pagliaro, M.; Ciriminna, R.; Kimura, H.; Rossi, M.; Pina, C. D.; *Angew. Chem., Int. Ed.* **2007**, *46*, 4434.
9. Stošić, D.; Bennici, S.; Sirotin, S.; Calais, C.; Couturier, J.; Dubois, J.; Travert, A.; Auroux, A.; *Appl. Catal., A* **2012**, *447-448*, 124.
10. Sung, K. H.; Cheng, S.; *RSC Adv.* **2017**, *7*, 41880.
11. Fernandes, A.; Ribeiro, M. F.; Lourenço, J. P.; *Catal. Commun.* **2017**, *95*, 16.
12. Talebian-Kiakalaieh, A.; Amin, N. A. S.; Zakaria, Z. Y.; *J. Ind. Eng. Chem.* **2016**, *34*, 300.
13. Ding, J.; Ma, T.; Cui, M.; Shao, R.; Guan, R.; Wang, P.; *Mol. Catal.* **2018**, *461*, 1.
14. Suprun, W.; Lutecki, M.; Haber, T.; Papp, H.; *J. Mol. Catal. A: Chem.* **2009**, *309*, 71.
15. Deleplanque, J.; Dubois, J.-L.; Devaux, J.-F.; Ueda, W.; *Catal. Today* **2010**, *157*, 351.
16. Estevez, R.; Lopez-Pedrajas, S.; Blanco-Bonilla, F.; Luna, D.; Bautista, F. M.; *Chem. Eng. J.* **2015**, *282*, 179.
17. Lopez-Pedrajas, S.; Estevez, R.; Blanco-Bonilla, F.; Luna, D.; Bautista, F. M.; *J. Chem. Technol. Biotechnol.* **2017**, *92*, 2661.

18. Liu, B.; Jiang, P.; Zhang, P.; Zhao, H.; Huang, J.; *C. R. Chim.* **2017**, *20*, 540.
19. Mohamed, F. S.; Kiwan, H. H.; Mostafa, M. R.; *Adsorpt. Sci. Technol.* **2002**, *20*, 131.
20. Lopez-Pedrajas, S.; Estevez, R.; Navarro, R.; Luna, D.; Bautista, F. M.; *J. Mol. Catal. A: Chem.* **2016**, *421*, 92.
21. Li, W.; Zhu, Y.; Guo, X.; Nakanishi, K.; Kanamori, K.; Yang, H.; *Sci. Technol. Adv. Mater.* **2013**, *14*, 045007.
22. Ma, T.; Ding, J.; Shao, R.; Xu, W.; Yun, Z.; *Chem. Eng. J.* **2017**, *316*, 797.
23. Hamid, S. B. A.; Daud, N. A.; Suppiah, D. D.; Yehya, W. A.; Sudarsanam, P.; Bhargava, S. K.; *Polyhedron* **2016**, *120*, 154.
24. Alhanash, A.; Kozhevnikova, E. F.; Kozhevnikov, I. V.; *Appl. Catal., A* **2010**, *378*, 11.
25. Gan, H.; Zhao, X.; Song, B.; Guo, L.; Zhang, R.; Chen, C.; Chen, J.; Zhu, W.; Hou, Z.; *Chin. J. Catal.* **2014**, *35*, 1148.
26. dos Santos, M. B.; Andrade, H. M. C.; Mascarenhas, A. J. S.; *Microporous Mesoporous Mater.* **2016**, *223*, 105.

Submitted: December 25, 2019
Published online: March 17, 2020